J. Phys.: Condens. Matter **11** (1999) 8035–8048. Printed in the UK PII: S0953-8984(99)05048-1

Reactivity and morphology of $(10\bar{1}\bar{2})$-faceted and (3×3)-reconstructed GaN$(000\bar{1})$ epilayers grown on sapphire(0001)

F S Tautz†§, S Sloboshanin†, U Starke†‡ and J A Schaefer†

† Institut für Physik, Technische Universität Ilmenau, PO Box 100565, D-98684 Ilmenau, Germany

‡ Lehrstuhl für Festkörperphysik, Universität Erlangen-Nürnberg, Staudtstrasse 7, D-91058 Erlangen, Germany

E-mail: tautz@physik.tu-ilmenau.de

Received 8 June 1999

Abstract. We have investigated structural and chemical properties of heteroepitaxial films of GaN on $Al_2O_3(0001)$ using low energy electron diffraction (LEED), x-ray photoelectron spectroscopy (XPS) and high resolution electron energy loss spectroscopy (HREELS). Depending on the preparation conditions, two faceted surfaces with different morphologies and a flat, (3×3)-reconstructed surface were obtained. For one of the faceted surfaces a $(10\bar{1}\bar{2})$ orientation of the facet planes could be determined. For a sample grown by metal–organic chemical vapour deposition (MOCVD) N-termination and $(000\bar{1})$ polarity could be established by a combination of HREELS and angle-resolved XPS. For a different sample grown by molecular beam epitaxy (MBE) the same $(000\bar{1})$ polarity could be identified, this time concluded from the observation of the (3×3) reconstruction in LEED, which moreover is shown to be Ga rich by the present XPS measurements. Furthermore, we find the $(000\bar{1})$ surface to be highly reactive, causing water from the residual gas to adsorb dissociatively. Finally, exposure to atomic hydrogen leads to the observation in HREELS of N–H and Ga–H stretching vibrations at 403 meV and 227–247 meV, respectively, as expected for a faceted surface. Based on these observations, a structural model for the facets is proposed.

1. Introduction

GaN and its ternary alloys have recently received considerable attention in view of their useful optoelectronic properties. Due to the direct band gap of GaN bright light-emitting diodes [1] and laser diodes [2] in the blue and ultraviolet range can be fabricated from this material. It is also possible to take advantage of the large band gap of GaN in the engineering of high temperature semiconductor devices [3]. One should expect that the performance of these devices can be further improved once even better epitaxial layers of the material can be grown. Growth methods which have been successfully applied so far are molecular beam epitaxy (MBE) and metal–organic chemical vapour deposition (MOCVD) on various substrates. For both of these techniques several fundamental issues concerning the growth process remain unresolved. First of all, the polarity of the material obtained is often unknown and indeed difficult to determine [4–7]. In fact, for the epitaxial polarity relationship on sapphire (Al_2O_3) substrates, contradicting reports have been given [8, 9]. Secondly, due to large lattice and

§ Corresponding author.

0953-8984/99/418035+14$30.00

thermal expansion misfit values, a high dislocation density is always present in heteroepitaxial layers [10]. An established method to improve the quality of heteroepitaxially grown layers is the generation of GaN buffer layers on Al_2O_3, as well as GaAs or 6H-SiC substrates prior to growth [11]. An improved control of the surface properties could not only enhance the quality of the epitaxial films grown on these buffer layers, but would also be beneficial for the homoepitaxial growth of layers on GaN bulk material which—at present at least—show a polarity dependent (rough) surface morphology [8, 12]. Smooth surfaces are of particular importance when layered structures such as in laser devices are fabricated. In the present paper we show that detailed studies of GaN surfaces can provide a better understanding of their atomic structure and reactivity, which in turn may facilitate a better control of the surface properties necessary to improve the growth results.

Sapphire is a substrate commonly used for heteroepitaxial growth of GaN. On its (0001) surface, the hexagonal wurtzite polytype (2H) of GaN can be grown epitaxially even though the lattice mismatch is 14.8% [10], provided a GaN buffer layer is grown first, on which the nucleation density for the subsequent layer growth is enhanced [13]. However, the growth direction, i.e. the polarity of GaN layers obtained on $Al_2O_3(0001)$, is still far from clear [4, 5]. This holds even more for the detailed surface structure of the GaN films obtained. In this paper we report new experiments probing the surface properties of GaN layers grown on $Al_2O_3(0001)$ by means of MOCVD. We present structural results as revealed by low energy electron diffraction (LEED) as well as chemical aspects, namely the interaction of these surfaces with gases, as revealed by high resolution electron energy loss spectroscopy (HREELS). In addition we use x-ray photoelectron spectroscopy (XPS) results to monitor the composition of the surfaces prepared. We show that after preparation in ultra-high vacuum (UHV) the MOCVD sample used in this study is primarily nitrogen terminated. However, the nominally hexagonal surface of the sample is faceted immediately after the initial preparation, such that also Ga dangling bonds exist. The clean faceted $(000\bar{1})$ surface is very reactive towards hydrocarbons and water (which dissociates) from the residual gas present in the UHV chamber. Hydrogen etches the initially well ordered facet planes, leaving behind an atomically rough GaN $(000\bar{1})$ surface. Finally, if the surface is heated in Ga flux it is possible to bypass the facetting and to obtain Ga-rich surfaces with (3×3) LEED symmetry as shown for an MBE grown sample.

2. Sample preparation and surface morphology

One of the samples studied in this work was grown by MOCVD in a horizontal flow reactor, which is inductively heated and operated at a pressure of 200 mbar. Ammonia and trimethylgallium are used as component precursors, while silane and biscyclopentadienyl magnesium provide Si and Mg dopants. Purified hydrogen is used as carrier gas. Growth on the $Al_2O_3(0001)$ substrate polished to optical grade was initiated at 500–600 °C by the formation of a low temperature GaN buffer layer, followed by epitaxial growth at 1040 °C, which was terminated after 2 to 4 μm had been grown.

After the growth process the sample was exposed to air for transfer to the analysis chamber, equipped with a Delta 0.5 HREEL spectrometer, an ErLEED two grid low energy electron diffraction optic and a hemispherical analyser for XPS. A first check of the surface condition of the sample, applied immediately after introduction into UHV, revealed a 1×1 LEED pattern. A HREELS spectrum recorded at this stage is shown in figure 1(a). Clearly the dominant features are the well known Fuchs–Kliewer surface phonon polariton (FK1) at 87.3 meV [14, 15] and its multiples (FK2 and FK3) at 174.6 and 262 meV, respectively. In addition, one observes a strong loss peak at 361 and a double peak at 444/453 meV. The strong peak

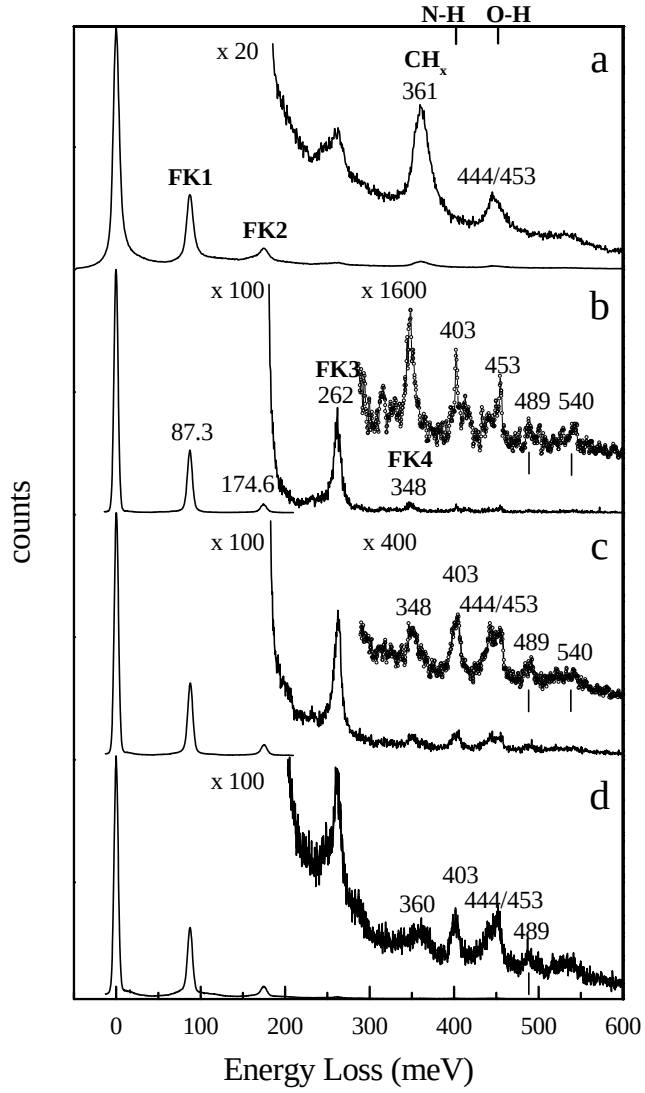

Figure 1. HREEL spectra obtained from the GaN(000$\bar{1}$) surface. Primary beam energy $E_0 = 10$ eV, incidence angle with respect to surface normal $\theta_i = 55°$. FWHM of the elastic peak amounts to 8.4 meV for (a) and 5.6 meV for (b) to (d). (a) sample as built in, (b) sputtered and subsequently annealed sample, spectrum recorded 20 min after preparation, (c) spectrum recorded after 2:15 h in UHV, (d) spectrum recorded after 19 h in UHV. FK = Fuchs–Kliewer phonon. In (b) and (c) the $\times 1600$ and $\times 400$ curves have been smoothed.

at 361 meV is due to CH_x vibrations [16], while the peak at 453 meV can be attributed to the O–H stretching vibration mode [16]. The origin of the 444 meV loss feature appears ambiguous. In figure 1(a), the 444 meV mode might be assigned to a combination loss of the CH_x mode and a Fuchs–Kliewer phonon. In the spectra shown in figures 1(c) and 1(d) we also observe a characteristic double structure at 444/453 meV. In these cases, however, it is impossible to assign the lower feature to a combination loss of a Fuchs–Kliewer phonon and the CH_x mode, since the latter, if present at all, has lower intensity than the 444 meV mode.

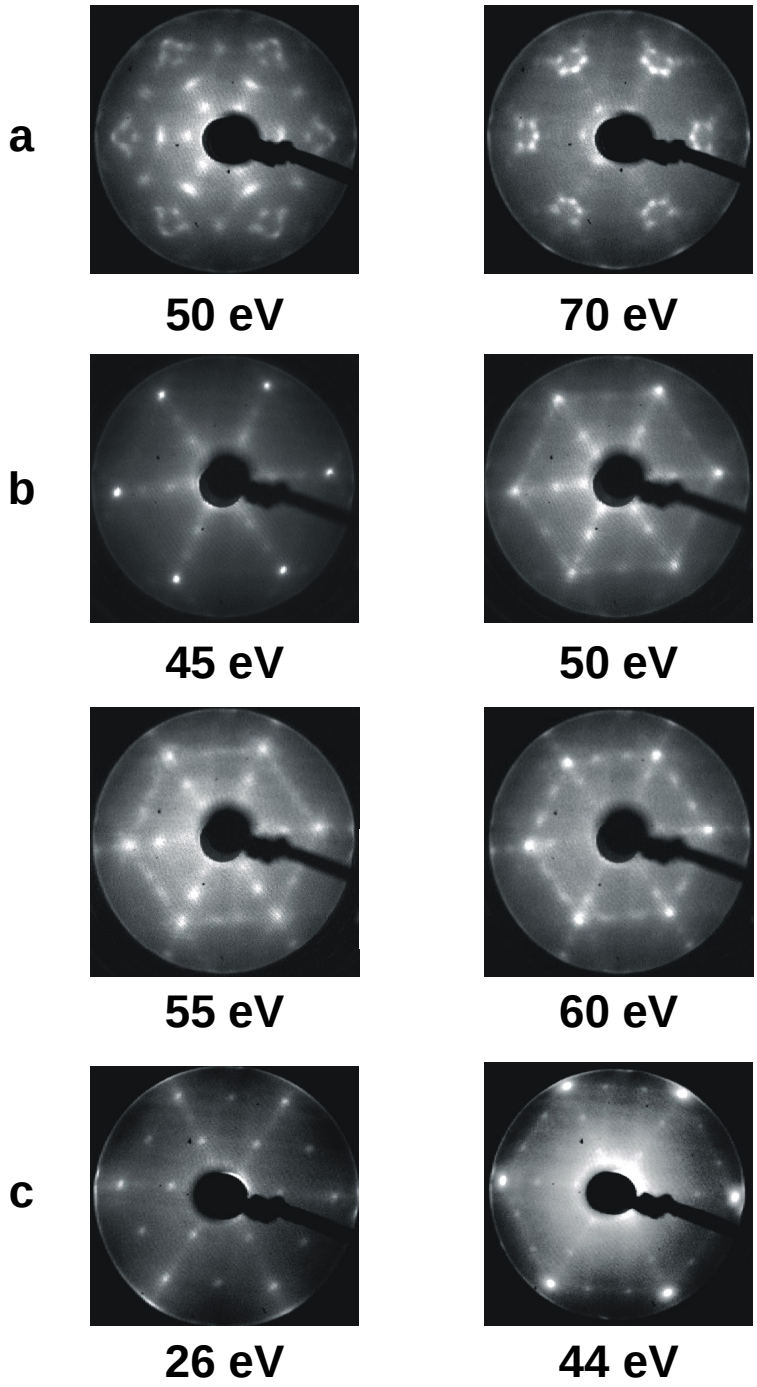

Figure 2. LEED patterns of differently prepared GaN(000$\bar{1}$) surfaces. (a) (1 × 1) symmetry with horseshoe facets appearing after heating to 1050 K, (b) (1 × 1) symmetry with (10$\overline{1}\overline{2}$)-type facets obtained on N-sputtered and annealed (950 K) surfaces. (c) (3 × 3) symmetry obtained on N-sputtered sample after 850 K annealing in Ga-flux. Images (a) and (b) have been obtained from the MOCVD sample, (c) from the MBE sample. Primary beam energies are indicated. Normal incidence was qualitatively adjusted.

The origin of the latter is therefore unclear, and may be related to two different adsorption sites of the OH group. Heating the sample to 950 K reduces the presence of hydrocarbons (disappearance of the 361 meV mode in HREELS) and leads to an increase of the elastic peak intensity in the HREELS experiment by almost two orders of magnitude (not shown here), indicating improved smoothness and order of the surface (the sample temperature was measured by a thermocouple in contact with the titanium support onto which the sample was clamped). However, it does not remove the carbon from the surface completely as can be concluded from glancing incidence XPS measurements (not shown here). Nevertheless, in contrast to sputter-cleaned surfaces discussed below, the sample is now passivated against uptake of CH_x and OH from the residual gas. Heating to even higher temperatures (1050 K) leads to a characteristic and reproducible facetting of the surface, identified in LEED by a characteristic horseshoe pattern (see figure 2(a)), which has also been reported in [17] and [18]. In order to remove the remaining contamination we employed nitrogen sputtering which was reported to produce stoichiometric surfaces [4], followed by subsequent annealing at 950 K. By this procedure the sample could be sufficiently cleaned as concluded from HREELS and XPS. The reduction of the CH_x contamination is particularly obvious in the HREEL spectrum in figure 1(b). Moreover, the strong background in HREELS present in figure 1(a) has disappeared, indicating good local order on these sputter-cleaned surfaces. These surfaces show a tendency to form different types of facets which occur in six equivalent planes as deduced from the star-type features in the LEED pattern (cf figure 2(b)). The tilt direction of the facets can be determined from the fact that the additional spots occur along the lines from the specular reflection towards the position of the first order spots of the unfaceted surface areas (see the sequence in figure 2(b)). The direction of the specular reflection measured for the tilted planes indicates a facet-normal angle of $\sim 40^\circ$ against the surface normal which is in reasonable agreement with a theoretical value of 43.2° for planes in $[10\overline{1}\overline{2}]$ orientation (by designating the facet as $(10\overline{1}\overline{2})$ rather than $(10\overline{1}2)$, we anticipate the polarity of the epitaxial layer as being $(000\bar{1})$. This is determined in the next section). It should be noted that the facet spots are not very sharp and vanish for rather broad energy ranges so that more sophisticated methods of determining the facet angle [19] cannot be applied. Of course, all six symmetry equivalent facet surfaces are present on the sample as immediately obvious from the sixfold rotational equivalency of the facet spots. Thus, one can envisage the faceted areas of the surface as either triangular (in two rotational orientations) or hexagonal and possibly truncated pyramids or pyramidal depressions.

We note that under many growth conditions samples show the formation of nanopipes and pinholes [20]. A systematic investigation of these defects using cross-sectional transmission electron microscopy (TEM) [21] has revealed that nanopipes and pinholes generally have V-shaped cross-section, the V-angle being ~ 60 or $\sim 90^\circ$. Note that $(10\overline{1}\overline{1})$ facets and $(10\overline{1}\overline{2})$ facets show theoretical V-angles of 56.1 and 93.6° respectively. Apparently, the $(10\overline{1}\overline{2})$ facet orientation, which we find on our surfaces as a result of the UHV preparation, also plays some role during the growth process in the formation of pinholes, indicating a certain propensity of the system towards this surface. It may even be the case that the facets of the present sample decorate planar defects of similar character as the pinholes. The horseshoe pattern also observed in this work (figure 2(a)) and in [17, 18] shows additional facetting apart from the three $(10\overline{1}\overline{2})$ directions, indicating a still more complex surface morphology. These horseshoe LEED patterns have been interpreted as indication of the existence of steps, and both step height and terrace width have been calculated from the LEED patterns [18]. We note that in the case of regular step arrays one can equally well speak of facets. Meanwhile, the fact that one observes high order diffraction spots belonging to these 'steps' points to a high degree of regularity of the step array. Therefore we prefer to speak of facets.

Table 1. Change of the XPS intensity ratios $r_1 = I_{Ga\ 2p}/I_{Ga\ 3d}$ and $r_2 = I_{Ga\ 2p}/I_{N\ 1s}$ as a function of detection angle relative to the surface normal. Experimental values are an average over six independent sample preparations. Standard deviation is given as error. Model calculations are based on exponential damping of photoelectrons during their escape from a layered structure which represents the wurtzite GaN crystal. Ga and N layer thicknesses of $d = 1.3$ Å have been chosen, four of these layers (i.e. two GaN bilayers) adding up to the c-axis lattice constant of 5.185 Å. Inelastic electronic mean free paths of $\lambda = 6$ Å, $\lambda = 16$ Å and $\lambda = 20$ Å were used for Ga $2p_{3/2}$, N 1s and Ga 3d electrons, respectively. The sensitivity of the results to the exact value of λ and d was checked, yielding the same qualitative behaviour for a broad range of values around the adopted ones.

	Calculated		
Intensity ratios	(0001)	$(000\bar{1})$	Experimental
$r_1(80^\circ)/r_1(0^\circ)$	1.19	0.57	0.6 ± 0.1
$r_2(80^\circ)/r_2(0^\circ)$	1.72	0.40	0.5 ± 0.1

Once a surface was faceted, we found it difficult to find preparation conditions under which the facetting could be removed. For that reason, we started on a fresh sample with a different preparation scheme. The new sample had been grown without nucleation layer in a plasma induced MBE process on sapphire at approximately 800 °C. After initial nitrogen sputtering the sample was annealed in Ga flux at 850 K. After annealing times of approximately one hour we found in LEED a (3×3) pattern (figure 2(c)). From its occurrence we can conclude that the MBE sample has $(000\bar{1})$ polarity [22], in agreement with a polarity assignment for MBE samples from the same source made on the basis of the x-ray standing wave technique [23].

3. Surface polarity

Figure 1(b) shows the HREEL spectrum of the surface subsequent to the treatment described above. The modes at 361, 444 and 453 meV have practically disappeared indicating a clean surface. Due to the improved quality of the surface (lower background, reduced peak broadening) three multiple losses (at 174.6, 262 and 348 meV) of the Fuchs–Kliewer phonon (87.3 meV) can be resolved. Weak N–H [24] and O–H stretching vibrations can be observed at 403 and 453 meV, respectively. The still weaker features at 489 and 540 meV correspond to combination losses of respectively the N–H and the O–H stretching vibration and a Fuchs–Kliewer phonon.

Subsequently left in UHV for some hours, the surface undergoes characteristic changes as monitored in the HREEL spectra shown in figures 1(c) and 1(d): both the O–H (453 meV) and the N–H peak (403 meV) increase in parallel, while the Ga–H vibration, which is expected around 230 meV, does not show a similar effect (note the different scaling factors in figures 1(b)–(d)). In figure 1(d) the FK4 can no longer be resolved from a neighbouring mode at ∼360 meV, the latter indicating that also CH_x has accumulated on the surface. Obviously, the surface is reactive to both water and hydrocarbons, and water adsorbs dissociatively, the products OH and H binding separately to the surface. Noteworthily, hydrogen predominantly binds to N and not to Ga, proving that the sample contains N-terminated areas.

Since it cannot be decided from HREELS alone whether these are terraces or facets, we additionally conducted glancing-angle XPS experiments and evaluated the integral intensities of N 1s, Ga 2p and Ga 3d lines at normal and 80° detection angle. The results are shown in table 1. By quoting $r_i(80^\circ)/r_i(0^\circ)$, where $r_1 = I_{Ga\ 2p}/I_{Ga\ 3d}$ and $r_2 = I_{Ga\ 2p}/I_{N\ 1s}$, rather than the intensity ratios r_1 and r_2 themselves, it is possible to compare to model

calculations without the necessity to know the energy dependent analyser transmission $T(E)$, the photoionization cross sections σ and the asymmetry factor $L(\gamma)$ which depends on the (here constant) angle γ between exciting photons and detected electrons. Table 1 also includes calculated values for these photoelectron ratios. These calculations are based on the following equation for the photoelectron intensity [25]:

$$I(\theta) = T(E)A(E)\sigma L(\gamma)\int_0^\infty c(z)\exp\left(-\frac{z}{\lambda\cos\theta}\right)\mathrm{d}z \tag{1}$$

where $c(z)$ is the depth-dependent concentration of atoms, A is the sample area being analysed, λ is the inelastic mean free path and θ is the detection angle measured with respect to the surface normal. In a layered structure where the concentration of a particular emitter is constant in the range $z_1 = nd$ to $z_2 = (n+1)d$, d being the layer thickness, the intensity of photoelectrons from this layer at the surface becomes:

$$I(\theta) = TA\sigma L\lambda\cos\theta\,\mathrm{e}^{-\frac{nd}{\lambda\cos\theta}}(1-\mathrm{e}^{-\frac{d}{\lambda\cos\theta}}). \tag{2}$$

If the GaN wurtzite crystal is modelled by alternating Ga and N layers perpendicular to the c-axis (and surface normal), one has to sum the contributions for each layer according to equation (2) until convergence is achieved. Both a (0001) and a $(000\bar{1})$ oriented bulk terminated crystal were thus simulated, the latter predicting intensity ratios in excellent agreement with experimental values. This result in combination with the direct evidence for N-termination provided by HREELS alone is good evidence that the (main) growth direction for the present sample is $(000\bar{1})$.

Of course, our model calculation does not take into account the presence of surface facetting. Therefore, the experiments should in principle be repeated on samples with flat surfaces. Unfortunately, the surface quality of currently available epilayers and/or the known preparation techniques do not allow such experiments at present. There is, however, a 'hand waving' argument explaining why the measured intensity ratios are apparently not affected by the presence of the facets. Firstly, the facet angle is about 40° such that 0 and 80° detection relative to the surface normal lead—to zeroth order—to identical escape angles *from the facets*. Secondly, we note that perpendicular to the facet planes the crystal lattice cannot be modelled by a layered structure (the terminating layer for example contains both N and Ga atoms, see figure 5). Therefore, beneath the facet surface the crystal is much better modelled by a homogeneous mixture of Ga and N atoms. In our model calculation, such a homogeneous system will *not* lead to angle dependent $r_i(80°)/ri(0°)$ ratios.

Simple analyses of photoelectron intensity in terms of direction cosines need to be taken with caution because of the possibility of intensity modulation through photoelectron diffraction. Usually the intensity is integrated over the azimuthal angle in order to average out photoelectron diffraction effects. Due to instrumental limitations, we could not carry out such a procedure. However, 2π-scans of the photoelectron intensity both from the N 1s and the Ga 3p levels in GaN$(000\bar{1})$ have been published [26] and do not show appreciable variation of intensity with azimuthal angle at 80° polar angle, so that one can be confident that the results of table 1 are not affected by photoelectron diffraction to a significant degree. Furthermore, we note that two independent intensity ratios are evaluated using three different core levels. Thus, with different electron energies employed, we would expect photoelectron diffraction to affect our results for these two intensity ratios differently, which is obviously not the case.

For several reasons we reject the possibility that N-sputtering artificially terminates a (0001) surface with an adlayer of nitrogen. Firstly, since we observe a (1×1) surface, this would mean a complete and unreconstructed monolayer of N on the Ga face of the topmost bilayer. In such a configuration, each N-atom would be onefold coordinated and

on an unreconstructed (1×1) phase have three dangling bonds if charge redistribution effects are neglected, a configuration which for obvious reasons would be highly unstable. Secondly, Bermudez [5] has compared the preparation of GaN surfaces by *in situ* deposition of Ga metal followed by thermal desorption with the N-sputtering and annealing method. No difference was found in Auger electron spectroscopy (AES), XPS, ultraviolet photoelectron spectroscopy (UPS) and electron energy loss spectroscopy (ELS), even for termination-sensitive quantities such as work function and band bending.

Using LEED and time-of-flight ion scattering and recoil spectroscopy (TOF-SARS) surfaces of (1×1) symmetry exhibiting both (0001) and $(000\bar{1})$ orientation were found for different GaN epilayers on sapphire $(11\bar{2}0)$ [27] and (0001) [9]. In agreement with the present results, it was also found there that the $(000\bar{1})$ surface shows a tendency towards hydrogen termination. Our observation of water dissociation explains the origin of hydrogen which in [27] was present on all $(000\bar{1})$ surfaces. In that study, the $(000\bar{1})$ surface appeared less reactive towards residual gas (carbon and oxygen components) than the (0001) surface, while the latter never took up as much hydrogen, even after long standing times, which confirms our main polarity assignment. In further agreement with the present work, Ahn *et al* [27] and Ponce *et al* [8] have observed a tendency towards facet formation during UHV annealing exclusively for the $(000\bar{1})$ GaN surface. Finally, a plateau and valley morphology, though somewhat irregularly shaped, has been found for MBE-grown GaN $(000\bar{1})$ on sapphire(0001) [22]. In this context it is worth mentioning that by wet chemical etching in basic aqueous solutions only the GaN $(000\bar{1})$ is attacked [28], a fact which has been used as a chemical means for polarity determination [22]. In fact, even though our faceted surface has unsaturated Ga atoms at the vacuum interface (see below), the water dissociation apparently takes place almost exclusively on the N-terminated areas. Photoelectron diffraction from GaN samples showing hexagonal columns, grown by MOCVD on sapphire(0001) without a buffer layer, has also shown N-termination of the surface [16]. In contrast to our results and those published in [9] and [27], different epitaxial GaN layers on Al_2O_3(0001) were monitored by convergent beam electron diffraction and exclusively showed (0001) orientation [8]. In ion channelling experiments, on the other hand, (0001) orientation was found for flat GaN films grown on (0001) sapphire, while rough pyramidal films tended to have small (0001) inversion domains in a $(000\bar{1})$ matrix [29]. Finally, first-principles calculations of surface properties have shown that 1×1 symmetries are only expected for the $(000\bar{1})$ orientation [30], a result consistent with our observation but contradicting the findings by Ahn *et al* [27]. However, in a recent publication [22] a pseudo-1×1 phase with satellites was identified on the (0001) Ga face, making a polarity assignment based on the occurrence of the (1×1) phase ambiguous. It should also be mentioned that the 1×1 phase on the $(000\bar{1})$ face is from a first-principles calculation thought to be terminated by a Ga-adlayer on top of the topmost N-face bilayer [30], while our experimental results are inconsistent with a *complete* Ga-termination. However, the hydrogenation experiments to be described in the next section show the formation of Ga–H bonds most likely even *before* the surface is etched. While it would thus be consistent with our HREELS experiments if the N-polar surface was *partially* Ga covered, the grazing angle XPS results limit the Ga coverage to much less than a monolayer (cf the section on the 3×3 phase below).

4. Surface hydrogenation

The polarity assignment can be further corroborated by atomic hydrogen adsorption experiments, using the hot filament technique. Recently, hydrogen adsorption studies have been performed both with TOF-SARS on polycrystalline GaN [31] and by temperature

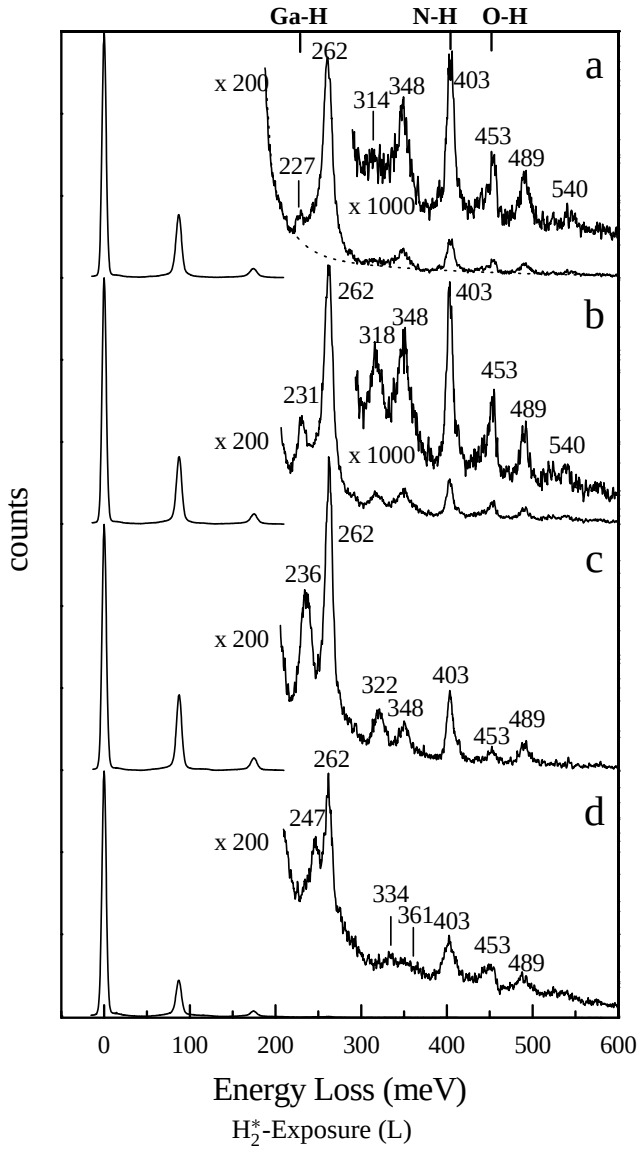

Figure 3. HREEL spectra for hydrogenated GaN surfaces prepared with (a) 2 L, (b) 10 L, (c) 50 L and (d) 2000 L hydrogen exposure. Experimental parameters as in figure 1. FWHMs of the elastic peaks range from 5.6 to 6.0 meV. All surfaces show 1×1 LEED symmetries. In (a) to (c) the (1×1) LEED pattern shows facets, while in (d) the facets have disappeared.

programmed desorption spectroscopy (TPD) on the hexagonal face of single-crystalline GaN grown by MOCVD on sapphire [32]. Not surprisingly, on polycrystalline samples adsorption on both N- and Ga-sites was observed. With respect to adsorption-site determination, the results of the TPD study were inconclusive. Here, we study hydrogen adsorption on the star-type faceted surface by HREELS. As shown in figure 3(a), even for low hydrogen exposures (2 Langmuir (= L)) the N–H vibration (403 meV) is now more intense than the O–H vibration (453 meV), indicating that hydrogen *directly* reacts with the N-terminated surface regions.

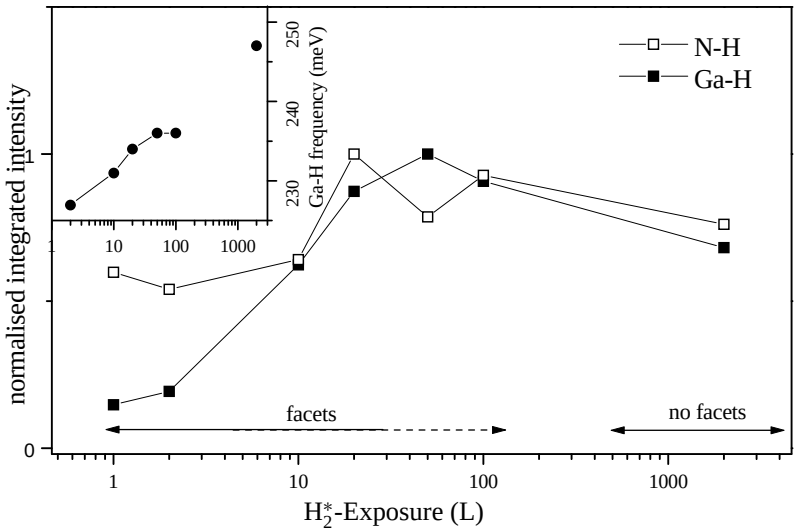

Figure 4. Integrated intensities of the Ga–H and N–H stretch frequencies in HREELS, normalized to the elastic peak and then plotted against hydrogen exposure in Langmuirs such that maximum intensity of each line corresponds to 1. Inset: Ga–H stretch frequency versus hydrogen exposure.

The presence of the O–H vibration, however, indicates that the surface still dissociates small amounts of water, either during the hydrogenation or afterwards. From 2 L onwards, the Ga–H mode at 227 meV together with its combination with a Fuchs–Kliewer phonon at 314 meV is discernable [33], but its intensity is considerably smaller than that of the N–H mode (figure 3(a)). The evolution of the integrated N–H and Ga–H intensities with H-exposure in the range 1 to 2000 L is plotted in figure 4, each normalized to maximum intensity, since the intensities of the vibrations of different surface molecules generally carry no quantitative information with regard to their relative abundance. Around 10 L hydrogen exposure the situation changes, and the Ga–H peak rises quickly to larger intensities than the N–H mode (figure 3(b) and 3(c)), while the latter's intensity barely changes, now indicating the preferred formation of Ga–H. Thereafter both peaks increase in intensity, eventually saturating in the range around 50 L (figure 4), before dropping off slightly at the highest exposures. While the LEED pattern still shows facetting of the surface up to 100 L, exposing the surface to 2000 L leads to a near complete disappearance of the facets which may be taken as indicating some kind of etching of the surface.

As far as the peak energies are concerned, the behaviour of the N–H and the Ga–H modes is very different. While the N–H mode shows no systematic frequency shift, the Ga–H mode shifts over the whole range of exposures studied here, starting at 227 meV and eventually occurring at 247 meV (inset to figure 4). Frequency shifts for surface adsorbed atoms or molecules are commonly observed if a strong dynamic or static dipole–dipole interaction between neighbouring adsorbate complexes exists [34]. Apparently this is the case *only* for the Ga–H mode. We note that in many cases the frequency shift is accompanied by a non-linear variation of the intensity with coverage, such that reliable estimates of the relative coverages become difficult.

Based on these observations, we thus propose the following model of the hydrogenation process. The N-terminated $(000\bar{1})$ terraces are hydrogenated first (figure 3(a)), which can be

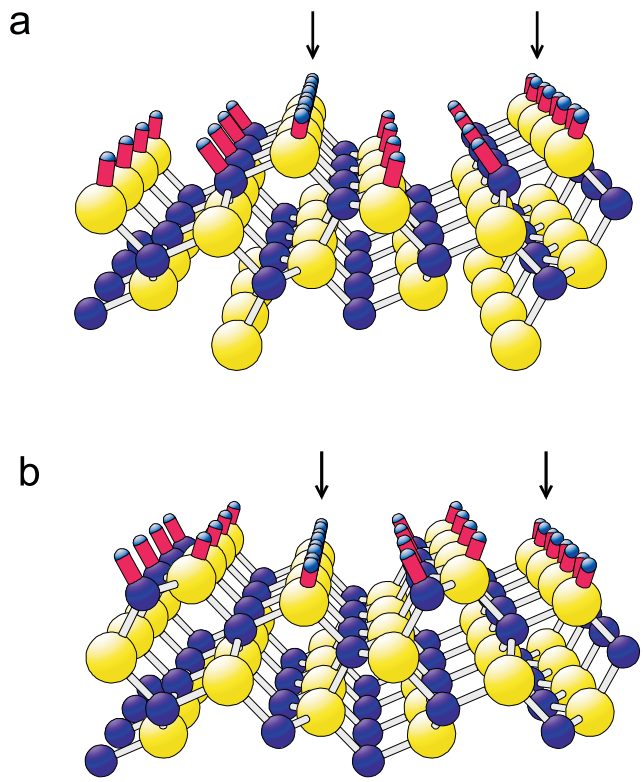

Figure 5. Atomic model of two possible $(10\bar{1}\bar{2})$ facet surfaces (a and b). Large spheres (light grey): Ga atoms, small spheres (black): N atoms. The surface is shown unreconstructed with all of its dangling bonds (dark grey). The arrows indicate rows of Ga atoms having two dangling bonds each, as well as the length of the surface unit mesh parallel to the projection plane $(11\bar{2}0)$.

understood in terms of the larger enthalpy of formation of the N–H bond as compared to the Ga–H bond [31]. The subsequent rise in the Ga–H intensity can be explained by saturation of Ga dangling bonds on the facet planes and possibly by the onset of etching on the terraces. In figures 5(a) and 5(b) we show sketches of the atomic arrangement of two feasible terminations of a $(10\bar{1}\bar{2})$ surface, the facet orientation deduced from LEED experiments. In both cases the surface contains N atoms with a single dangling bond and two types of Ga atom, one with a single and another (indicated by the arrows) with a pair of dangling bonds. It is not surprising, therefore, that the unetched, still faceted $(000\bar{1})$ surface can accommodate Ga–H species, as seen in the spectrum of e.g. figure 3(b). Because of their higher reactivity it is expected that the double-valent Ga atoms are hydrogenated before the monovalent ones, the former eventually leading to N_2GaH_2 complexes as compared to N_3GaH for the latter. The number of backbonds in a N_2GaH complex may explain the initially relatively low Ga–H stretching frequency of 227 meV, if compared to the calculated value of 250 meV for an N_3GaH unit on the $(10\bar{1}\bar{0})$ GaN surface [35], since it is well known that backbonds to electronegative partners stiffen the stretching vibrations [36].

The strong coverage dependent frequency shift of the Ga–H line is also observed for GaAs(100) [33] and GaAs(111) [37]. While we cannot at present give a final explanation for this phenomenon, the shift does fit in well with our model if we assign it to the dense packing

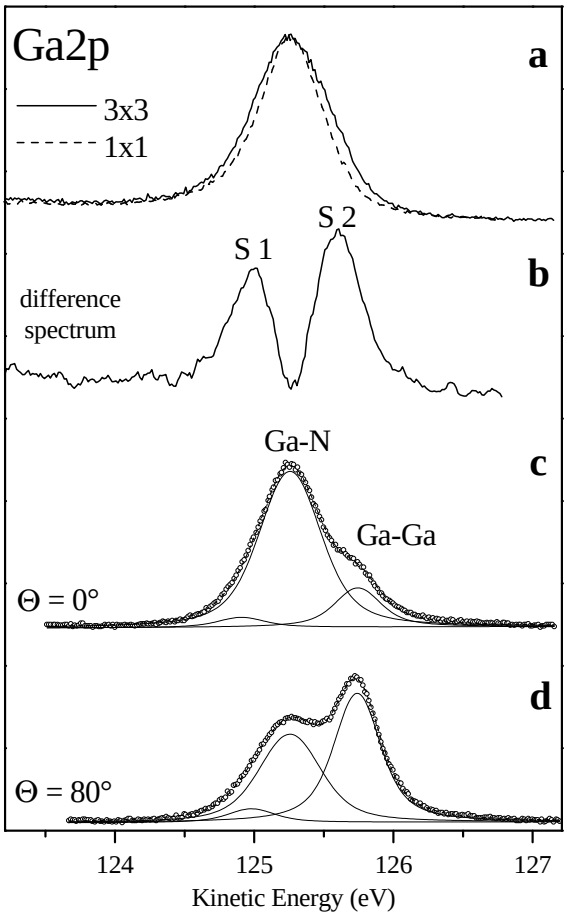

Figure 6. XPS spectra of the Ga 2p line of the GaN$(000\bar{1})$ surface of the MBE grown sample: (a) experimental spectra for the 3×3 (solid) and 1×1 (dashed) phases, (b) difference spectrum $(3 \times 3) - (1 \times 1)$, (c) spectrum detected at 0° from a surface with excess Ga (no 3×3 LEED pattern visible), (d) as (c) but 80° detection.

of Ga–H bonds along the rows of double-valent Ga atoms on the facets (cf arrows in figure 5) and the resultant strong interaction between neighbouring bonds. This could be responsible at least for the shift from 227 meV to 236 meV at 50 L and 100 L exposures. Note that for the highest Ga–H intensities at 50 and 100 ML, the frequency no longer shifts (figure 4). From then on the interpretation of the shift is more difficult. While it is not uncommon for the intensity to saturate or even fall off while the frequency keeps shifting, a behaviour which may also apply to the present case (figures 3(c) and 3(d)), the gradual disappearance of the facets in LEED points towards major topographic changes of the surface. It is therefore also conceivable that the Ga–H line position at 247 meV indicates a different hydrogen adsorption site on the etched surface. In this context we moreover note a considerable increase of the diffuse background scattering in HREELS characteristic for disordered surfaces (figure 3(d)) and a broadening of the N–H vibration (figure 3(d)) which may also indicate the simultaneous occupation of different N–H adsorption sites on an etched surface.

5. (3 × 3) phase

Finally, we note the appearance of a (3 × 3) phase on our MBE grown sample. Several superstructure phases have been observed by scanning tunnelling microscopy (STM) on both hexagonal surfaces of GaN [22, 30]. The (3 × 3) phase only occurs on GaN $(000\bar{1})$. In figure 6(a) we show XPS intensities for Ga 2p emission compared for the initial (1 × 1) phase with facets and the (3 × 3) phase which clearly is Ga enriched. To further exemplify this observation we inspect a difference spectrum of the two phases as shown in figure 6(b). The Ga 2p spectrum from the (3 × 3) phase obviously contains two additional components denoted S1 and S2 in the figure. In order to identify these components we have evaporated an excess of Ga onto the 3 × 3 surface such that the 3 × 3 LEED patterns disappears. The corresponding spectra at 0 and 80° detection angle are shown in figure 6(c) and (d). They allow us to identify S2 with Ga in the environment of metallic Ga. S1 could thus be connected to Ga atoms terminating the uppermost GaN bilayer of the $(000\bar{1})$ surface. For the 3 × 3 surfaces we have also evaluated the intensity ratios $r_i(80^\circ)/r_i(0^\circ)$ as discussed above. The experimental ratios determined are $r_1(80^\circ)/r_1(0^\circ) = 0.8$ and $r_2(80^\circ)/r_2(0^\circ) = 1.4$. These values are in between the two extremes of complete N- and complete Ga-termination, a result which is consistent with Ga-adatom coverage. However, the theoretical evaluation of specific adatom models is beyond the scope of the currently employed model calculation.

References

[1] Nakamura S, Senoh M, Iwasa N and Nagahama S 1995 *Japan. J. Appl. Phys.* 2 **34** L797
Nakamura S, Senoh M, Iwasa N, Nagahama S, Yamada T and Mukai T 1995 *Japan. J. Appl. Phys.* 2 **34** L1332
[2] Nakamura S, Senoh M, Nagahama S, Iwasa N, Yamada T, Matsushida T, Kiyuki H, Sugimoto Y 1996 *Japan. J. Appl. Phys.* **35** L74
Nakamura S, Senoh M, Nagahama S, Iwasa N, Yamada T, Matsushida T, Kiyuki H and Sugimoto Y 1996 *Appl. Phys. Lett.* **68** 2105
[3] Khan M A, Kuznia J N, Bhattarai A R and Olson K T 1993 *Appl. Phys. Lett.* **62** 1786
Imari S B, Rowland L B, Kruppa W, Kelna G, Doverspike K and Gatskill D K 1994 *Electron. Lett.* **30** 1248
[4] Wu C I, Kahn A, Taskar N, Dorman D and Gallagher D 1998 *J. Appl. Phys.* **83** 4249
[5] Bermudez V M 1996 *J. Appl. Phys.* **80** 1190
[6] Dhesi S S, Stagarescu C B, Smith K E, Doppalapudi D, Singh R and Moustakas T D 1997 *Phys. Rev.* B **56** 10 271
[7] Rapcewicz K, Nardelli M B and Bernholc J 1997 *Phys. Rev.* B **56** R12 725
[8] Ponce F A, Bour D P, Young W T, Saunders M and Steeds J W 1996 *Appl. Phys. Lett.* **69** 337
[9] Sung M M, Ahn J, Bykov V, Rabalais J W, Koleske D D and Wickenden A E 1996 *Phys. Rev.* B **54** 14 652
[10] Ponce F A 1998 *Group III Nitride Semiconductor Compounds* ed B Gil (Oxford: Oxford University Press) p 123
[11] Yoshida S, Misawa S and Gonda S 1983 *Appl. Phys. Lett.* **42** 427
Amano H, Sawaki N, Akasaki I and Toyoda Y 1986 *Appl. Phys. Lett.* **48** 353
Nakamura S 1991 *Japan. J. Appl. Phys.* **30** L1705
[12] Ivantsov V A, Sukhoveev V A and Dimitriev V A 1997 *Mater. Res. Soc. Symp. Proc.* vol 468 (Pittsburgh, PA: Materials Reseach Society) p 143
Melnik Yu V, Vassilevski K V, Nikitina I P, Babinin A I, Davydov Yu V and Dimitriev V A 1997 *MRS-Internet J. Nitride Semicond.* **2** 39
[13] Hiramatsu K, Itoh S, Amano H, Akasaki I, Kuwano N, Shiraishi T and Oki K 1991 *J. Crystal Growth* **115** 628
Nakamura S 1991 *Japan. J. Appl. Phys.* **30** 1620
[14] Grabowski S P, Kampen T U, Nienhaus H and Mönch W 1998 *Appl. Surf. Sci.* **123/124** 33
[15] He Z Q, Ding X M, Hou X Y and Wang X 1994 *Appl. Phys. Lett.* **64** 315
[16] Herzberg G 1991 *Molecular Spectra and Molecular Structure* vol II (Malabar, FL: Krieger) p 195
[17] Bermudez V M, Jung T M, Doverspike K and Wickenden A E 1996 *J. Appl. Phys.* **79** 110
[18] Janzen O, Hahn Ch, Kampen T U and Mönch W 1999 *Eur. Phys. J.* B **7** 1
[19] Tucker C W 1967 *J. Appl. Phys.* **38** 1988

[20] Qian W, Rohrer G S, Skowronski M, Doverspike K, Rowland L B and Gaskill D K 1995 *Appl. Phys. Lett.* **67** 2284
Liliental-Weber Z, Ruvimov S, Suski T, Ager III J W, Swider W, Washburn J, Amano H, Akasaki I and Imler W 1996 *Mater. Res. Soc. Symp. Proc.* vol 423 (Pittsburgh, PA: Materials Research Society) p 487
[21] Liliental-Weber Z, Chen Y, Ruvimov S, Washburn J 1997 *Phys. Rev. Lett.* **79** 2835
[22] Smith A R, Feenstra R M, Greve D W, Shin M S, Skowronski M, Neugebauer J and Northrup J E 1998 *Appl. Phys. Lett.* **72** 2114
[23] Kazimirov A, Scherb G, Zegenhagen J, Lee T L, Bedzyk M J, Kelly M K, Angerer H and Ambacher O 1998 *J. Appl. Phys.* **84** 1703
[24] Herzberg, cited in [16], reports a group frequency =N–H of 415 meV, where these so-called group frequencies commonly are accurate to ± 100 cm^{-1} (13 meV). Franchy R, Schmitz G, Gassmann P, Bartolucci F 1997 *Appl. Phys.* A **65** 551 report an N–H stretch frequency of NH units bound to the NiAl(111) surface of 410 meV
[25] Seah M P and Dench W A 1995 *Surf. Interface Anal.* **1** 2
Cumpson P J 1995 *J. Electron. Spectrosc. Relat. Phenom.* **73** 25
[26] Denecke R, Morais J, Wetzel C, Liesegang J, Haller E E and Fadley C S 1997 *Mater. Res. Soc. Symp. Proc.* vol 468 (Pittsburgh, PA: Materials Reseach Society) p 143
[27] Ahn J, Sung M M, Rabalais J W, Koleske D D and Wickenden A E 1997 *J. Chem. Phys.* **107** 9577
[28] Seelmann-Eggebert M, Weyher J L, Obloh H, Zimmermann H, Rar A and Porowski S 1997 *Appl. Phys. Lett.* **71** 2635
[29] Daudin B, Rouviere J L and Arlery M 1996 *Appl. Phys. Lett.* **69** 2480
[30] Smith A R, Feenstra R M, Grewe D W, Neugebauer J and Northrup J E 1997 *Phys. Rev. Lett.* **79** 3934
[31] Chiang C M, Gates S M, Bensaoula A and Schultz J A 1995 *Chem. Phys. Lett.* **246** 275
[32] Shekhar R and Jensen K F 1997 *Surf. Sci.* **381** L581
[33] Schaefer J A *et al* 1991 *Physica* B **170** 481
Schaefer J A, Allinger Th, Stuhlmann Ch, Beckers U and Ibach H 1991 *Surf. Sci.* **251/252** 1000 report a Ga–H stretching frequency on GaAs(100) of between 230 and 236 meV, depending on hydrogen exposure
[34] See e.g. Ibach H and Mills D 1982 *Electron Energy Loss Spectroscopy* (New York: Academic)
[35] Northrup J E, Di Felice R and Neugebauer J 1997 *Phys. Rev.* B **56** R4325
[36] Schaefer J A, Frankel D, Stucki F, Göpel W and Lapeyre'G J 1984 *Surf. Sci.* **139** L209
[37] Frankel D J *et al* 1985 *J. Vac. Sci. Technol.* B **3** 1093 report a Ga–H stretching frequency on GaAs(111) (Ga face) of between 224 and 234 meV depending on hydrogen exposure.